Research Square

Preprints are preliminary reports that have not undergone peer review.
They should not be considered conclusive, used to inform clinical practice,
or referenced by the media as validated information.

The physicochemical properties of RS_3 from different staple grains and their effects on the quality of low-GI extruded rice

Songheng Wu
Shanghai Academy of Agricultural Sciences
Haoyu Si
Shanghai Academy of Agricultural Sciences
Kai Zhu
Shanghai Academy of Agricultural Sciences
Xing Jia
Shanghai Academy of Agricultural Sciences
Qi Zheng
Shanghai Shuneng Irradiation Technology Co. Ltd
Wenhui Tian
Shanghai Shuneng Irradiation Technology Co. Ltd
Yuemei Zhang
Shanghai Academy of Agricultural Sciences
Hongzhu Chen
Shanghai Xincheng Food Co., Ltd
Ruihan Lin
Methuselah (Shanghai) Medical Technology Co., Ltd
Yongjin Qiao
Shanghai Academy of Agricultural Sciences
Yi Zhang
zhangyi@saas.sh.cn

Shanghai Academy of Agricultural Sciences

Research Article

Keywords: resistant starch, staple grain, extruded rice, physicochemical characteristics, digestive characteristics

Posted Date: November 4th, 2026

DOI: https://doi.org/10.21203/rs.3.rs-11315589/v1

License: This work is licensed under a Creative Commons Attribution 4.0 International License. Read Full License

Additional Declarations: No competing interests reported.

Abstract

Resistant starch type 3 (RS_3), due to its enzymatic resistance and thermal stability, has emerged as an ideal ingredient for developing low glycemic index (GI) foods. RS_3 from different staple grains (wheat, rice, and maize) was prepared in this study, and their structural and physicochemical properties were analyzed. Then, the RS_3 was blended with rice flour and other ingredients and processed into extruded rice. The results show that RS content and solubility (31.65–37.90%) of RS_3 were significantly increased, while swelling power (5.81–6.90 g/g) was lower than that of the native starch. Among them, maize RS_3 exhibited the highest RS content (35.28%). The extruded rice fortified with RS_3 showed a lower estimated GI, with the maize RS_3 formulation achieving the lowest value (45.88). These findings suggest that RS_3 can enhance the quality of extruded rice while reducing its glycemic potential, providing new insights for the development of low-GI foods.

1. Introduction

China currently has the highest number of individuals diagnosed with diabetes worldwide, exceeding 140 million cases and accounting for over a quarter of the global total (Deng et al., 2024). Although current pharmacological treatments cannot fully cure diabetes, dietary interventions hold significant potential for preventing or delaying its onset (Noori et al., 2023; Walker et al., 2010). Driven by shifting lifestyle patterns, there is a growing demand for functional foods featuring a low glycemic index (GI), weight management benefits, and improved gut health. Low-GI foods play a vital role in curbing appetite, enhancing satiety, and preventing overeating (Stewart et al., 2018).

Resistant starch (RS) is a form of dietary fiber that escapes digestion and absorption in the small intestine, passing directly into the large intestine where it is fermented by intestinal microorganisms. It offers significant potential health benefits, including blood glucose regulation, gut microbiota modulation, and weight management. RS is naturally abundant in whole grains, legumes, and cooked-and-cooled staple foods, with numerous studies confirming a strong negative correlation between RS content and glycemic index (GI) levels (Schmidt et al., 2023). Based on its properties and mechanisms of formation, RS is categorized into five types: RS_1 (physically entrapped starch), RS_2 (nongelatinized native starch granules), RS_3 (retrograded amylose), RS_4 (chemically modified starch), and RS_5 (amylose–lipid complexes) (Q. Liu et al., 2025). Among these, RS_3, which is often referred to as retrograded starch, is formed when gelatinized starch cools, allowing amylose molecules to reassociate via intermolecular hydrogen bonds into a dense crystalline structure. This compact network restricts amylase access to the substrate, rendering RS_3 highly resistant to enzymatic hydrolysis. Due to its superior thermal stability and eco-friendly preparation, RS_3 shows clear advantages for low-GI food manufacturing, with staple grains serving as ideal raw materials owing to their abundance and high starch content (Si et al., 2024). Recent studies demonstrate this potential across various grains: Zhang et al. achieved an RS_3 content of 58.87% by debranching maize starch with pullulanase (Si et al., 2024); Arp et al. prepared RS_3 from native wheat starch, significantly reducing digestibility and lowering the estimated glycemic index (eGI) to 66% (Arp et al., 2020); and Liao et al. synthesized RS_3 from rice flour, markedly improving both RS content and thermal stability while blunting the glycemic response (Liao et al., 2016).

Rice is a primary staple grain for a large portion of the Asian population. However, because rice starch is rapidly digested and absorbed, it often triggers sharp postprandial blood glucose spikes, making natural rice unsuitable for individuals with diabetes (Liao et al., 2016). Extrusion processing is an advanced technology that integrates mixing, thermal treatment, sterilization, and molding, and is widely applied in the food industry. By incorporating targeted ingredients tailored to specific nutritional requirements, extrusion allows for the creation of high-value-added foods, offering practical solutions for specialized dietary needs (Gong et al., 2026). Accordingly, the development of extruded

rice aims to overcome the nutritional limitations of natural rice by tailoring formulations for target populations or specific health scenarios. Among these applications, low-GI extruded rice enriched with resistant starch shows significant promise for managing hyperglycemia and diabetes. For instance, Zhang et al. formulated recombinant rice by blending rice flour with RS_4, resistant dextrin, konjac powder, and polyglycerol ester, successfully reducing its predicted glycemic index (Y. Zhang, 2022). However, the harsh extrusion environment—characterized by high temperatures, elevated pressure, and strong shear forces—transforms moist raw materials into a molten mass, which can compromise the enzymatic resistance of RS (M. Li et al., 2026). Compared to other RS types, RS_3 is physically produced from natural starches, exhibiting superior thermal stability, enzymatic resistance, and eco-friendliness, making its application in functional extruded rice highly promising. Nevertheless, studies investigating the direct incorporation of RS_3 into extruded rice for low-GI food development remain limited. Furthermore, the high-temperature extrusion process alters the structural and sensory attributes of extruded rice, rendering its quality distinct from that of natural rice. While current research has extensively focused on optimizing processing parameters, comprehensive evaluations of product quality attributes remain sparse. In particular, a thorough assessment of microstructure, textural profile, and eating quality for extruded rice is critical, not only for refining manufacturing parameters, but also for enhancing the overall quality and market competitiveness of RS_3.

This study aimed to investigate the effects of RS_3 derived from various staple grains on the cooking, textural, and pasting properties of extruded rice. Specifically, to enhance the preparation efficiency of rice-based RS_3, a high-amylose variety (Youtang Rice No.2) was selected as the raw material. Additionally, in vitro digestion experiments were conducted to evaluate eGI values and explore the potential of RS_3 in improving enzymatic resistance and blunting the glycemic response of extruded rice. The findings are expected to provide a scientific foundation for the high-value utilization of staple food resources, facilitate the development of low-GI functional rice, and offer novel dietary perspectives for individuals with chronic metabolic diseases.

2 Materials and methods

2.1 Materials

The grains used for extracting starch and preparing RS_3 were provided by the Shanghai Academy of Agricultural Sciences and included Wheat (Hetao flatlands red skin wheat), Rice (Youtang Rice No.2), and Maize (JD39). Fungal α-amylase (100000 U/g) and DNS reagent were purchased from Solarbio Science & Technology Co., Ltd. (Beijing, China). Pullulanase and Glucose standard were purchased from Macklin Biochemical Technology Co., Ltd. (Shanghai, China). Resistant starch assay kit was purchased from Megazyme International Ireland Ltd. Pepsin (porcine stomach mucosa, 30000 U/g), Glucoamylase and pancreatic α-amylase (≥ 5 U/mg) were purchased from Yuanye Bio-Technology Co., Ltd. (Shanghai, China). Papain (6000 U/mg) was purchased from Sinopharm Chemical Reagent Co., Ltd. (Shanghai, China). Soy proteins were purchased from Zhongsen Biotechnology Co., Ltd. (Shandong, China). Mono-and diglycerides of fatty acids were purchased from Maiyoutian Trading Co., Ltd. (Henan, China). Regular rice flour, chickpea flour and highland barley flour were purchased at a local market in Shanghai, China. All other chemicals were of analytical grade.

2.2 Starch extraction

To minimize the influence of different extraction methods on RS_3 preparation, Starches of wheat, rice, and maize were all extracted by alkaline method based on Romero-Bastida et al. with appropriate modifications (Romero-Bastida et al., 2005). A total of 50 g of wheat, rice and maize were washed and soaked in deionized water at 1:5 (*w*/*v*) ratio for 24 h. The soaked grains were then homogenized and centrifuged at 8000 rpm for 10 min. The precipitate was subsequently

soaked in 0.2% NaOH solution at a ratio of 1:5 (*w*/*v*) for 48 h, with the alkaline solution changed every 24 h. The mixture was passed through a 100-mesh sieve and repeatedly washed with deionized water until the pH approached neutrality. The precipitate was evenly stirred in 5 times the volume of deionized water to adjust the pH to 6, and 0.5 g papain was added to the mixture, then stirred at 50℃ for 5 h to remove the protein. After another round of centrifugation (8000 rpm, 10 min), the surface precipitate was scraped off. After freeze-drying, wheat, rice and corn starch with purity of more than 90% were obtained through 100 mesh sieve and stored in the dryer.

2.3 Preparation of RS_3

Refer to the method of Zhang et al. with appropriate modifications (H. Zhang et al., 2013). The starch milk was prepared with a ratio of material to liquid of 1:4. The pH was adjusted to 6 and then stirred at 80℃ for pre-gelatinization for 20 min. Fungal α-amylase was added at a concentration of 4 U/g, and enzymatic hydrolysis was carried out at 50℃ for 15 min. The mixture was treated at 95℃ for 20 min and cooled to room temperature. pH was then adjusted to 5, the amount of Pullulanase was 30 U/g, followed by enzymatic hydrolysis at 46℃ for 12 hours. The enzyme was then inactivated by heating at 95℃ for another 20 min, and cooled to room temperature. Afterward, the sample was stored at 4℃ for 24 h. The RS samples were purified by sugar removal, washed with 95% ethanol, dried and sieved with 100 mesh to obtain the RS_3 samples.

2.4 Physical properties of RS_3

2.4.1 RS content

Resistant starch assay kit (MK-RSTAR, Megazyme) was used to determine the RS content of RS_3 from wheat, rice and maize. All experiments were conducted following the procedures provided in the technical bulletins of the respective assay kits.

2.4.2 Swelling power and solubility

Measured according to the method described by Xing et al., with some modifications (Xing et al., 2017). Starches were dispersed in distilled water at a ratio of 1:25 (*w*/*v*) to prepare a starch suspension. The suspension was heated at 95℃ for 30 min with continuous stirring. After cooling to room temperature, the mixture was centrifuged at 5000 r/min for 25 min. The supernatant was transferred and evaporated at 105℃. The mass of the sediment remaining in the centrifuge tube was measured. Swelling power and solubility were calculated by the equation below:

$$\text{Swelling power } (\text{g/g}) = \frac{\text{P}}{\text{W}}$$

1

$$\text{Solubility } (\%) = \frac{\text{A}}{\text{W}} \times 100 \qquad (2)$$

where P is the weight of the sediment, W is the dry weight of starches, and A is the weight of the supernatant after drying.

2.5 Physical properties of RS_3

2.5.1 Fourier transform infrared (FTIR) spectroscopy

Starches were analyzed by Nicolet iS5 infrared spectrometer (Thermo Fisher Scientific Inc., USA) at a wavenumber range of 500–4000 cm^{-1} with a resolution of 4 cm^{-1} (Pang et al., 2024).

2.5.2 X-ray diffraction (XRD)

Starches were analyzed using a D8 ADVANCE Da Vinci multifunctional X-ray diffractometer (Bruker Corporation, Germany) to characterize their crystalline structure. The measurements were conducted at a voltage of 40 kV and a current of 44 mA. The scanning range was set from 5° to 35° (2θ) with a scanning rate of 4°/min.

2.6 Physicochemical and digestive properties of extruded rice

2.6.1 Preparation of extruded rice

The Youtang rice flour was mixed with RS_3 from different main food grains, chickpea flour, highland barley powder, soybean protein and mono-diglycerol fatty acid ester. The water content of the final mixture was 30%. Extruded rice was prepared using a Process 11 - parallel twin-screw extruder (Thermo Fisher Scientific Inc., USA) under the following barrel zone temperatures: 50℃, 60℃, 90℃, 100℃, 100℃, 100℃, 100℃, and 100℃. The screw speed was set at 43 r/min. After extrusion, the samples were cooled to room temperature and air-dried at 45℃ until a constant weight was achieved. The final formulation consisted of 50% Youtang rice flour, 19.25% RS_3 prepared from wheat (ER-2), rice (ER-3), or maize (ER-4), 10% chickpea flour, 10% highland barley flour, 10% soy protein, and 0.75% mono- and diglycerides of fatty acids. The control group, designated as ER-1, was prepared using regular rice flour instead of RS_3.

2.6.2 Scanning electron microscopy (SEM)

A small amount of sample was evenly mounted onto conductive adhesive tape. After gold sputtering, the particle morphology was observed and recorded at magnifications of 300× under an accelerating voltage of 2.0 kV by TM 4000 + SEM (Hitachi, Japan).

2.6.3 Cooking quality

The cooking quality of the extruded rice samples was determined following the method of Luo et al. with appropriate modifications (Luo et al., 2022). A specific weight of rice grains was cooked in boiling water at a ratio of 1:10 (*w*/*v*). At regular intervals, a few grains were removed and pressed between glass plates for visual inspection. Cooking was considered complete when more than 90% of the grains showed no visible opaque core. Subsequently, the samples were simmered for an additional 2 min to ensure full doneness. This cooking duration was defined as the optimal cooking time for each sample.

2.6.3.1 Water absorption rate

A specific weight of rice was placed into a non-woven fabric bag, and its initial weight was recorded. The sample was then steamed, and upon reaching the predetermined cooking time, the bag was removed and drained. After cooling the sample to room temperature and ensuring that dripping had completely ceased, surface moisture was carefully removed using filter paper. Then, the sample was weighed and recorded before and after cooking, and the water absorption was calculated.

2.6.3.2 Cooking loss rate

The weight of the container was measured in advance. After extruded rice was cooked, the cooking water was poured into the container, which was then placed in an oven and dried at 105℃ until a constant weight was achieved. After

cooling the container to room temperature, its final weight was recorded. The cooking loss per gram of extruded rice was calculated as a percentage.

2.6.4 Sensory evaluation

Sensory evaluation of the extruded rice samples was conducted by a panel of 10 members (5 males and 5 females). Prior to each sensory session, the panelists received detailed instructions regarding the evaluation criteria and parameters. Each panelist was presented with four extruded rice samples, which were randomly coded with symbols and served in a randomized order to minimize bias. Water was provided to each panelist for palate cleansing between samples. The evaluation was performed based on five attributes: odor, appearance structure, palatability, taste, and cold rice texture.

2.6.5 Pasting properties

Precisely 3.5 g of extruded rice flour (sieved through a 100-mesh screen) was weighed into a container and mixed thoroughly with 25 mL of deionized water. The mixture was then analyzed using RVA-TecMaster Rapid Visco Analyzer (RVA, Perten Instruments Co., Ltd., Sweden). The stirring speed was set to 960 r/min for the first 10 s, and then maintained at 160 r/min until the end of the measurement.

2.6.6 Textural properties

The textural properties of the extruded rice were determined by TA.XT plus texture analyzer (Stable Micro Systems Ltd., UK) based on the method of Wu et al. and appropriate modifications were made (Wu et al., 2016). Three grains of extruded rice were taken and placed on the platform after cooking. The probe was P/36R; the pre-test speed, the test speed and the test speed were set to 2 mm/s, 1 mm/s and 1 mm/s; the compression deformation rate was 35%, and the trigger force was 5 g.

2.6.7 eGI

The method was modified based on the procedures described by Ratnaningsih and Simsek (Ratnaningsih et al., 2020; Simsek & El, 2012). 50 mg of extruded rice flour was accurately weighed with 10 mL HCl-KCl buffer at pH 1.5, and 0.2 mL pepsin solution was added and incubated at 40°C for 1 h. After a TRIS-Maleic acid buffer at pH 6.9 was used to set the volume to 25 mL, 5 mL pancreatic α-amylase solution was added and incubated at 37°C for 3 h. Enzymatic hydrolysates were collected at 0, 30, 60, 90, 120 and 180 min, and the water bath was inactivated for 2 min. To each aliquot, 1 mL of 0.4 M sodium acetate buffer (pH 4.75) and 30 μL of glucoamylase were added. The mixtures were then incubated at 60°C for 45 min. The hydrolysis rate of starch was determined by DNS colorimetry. The hydrolysis index (HI) of extruded rice was obtained by calculating the area under the curve (AUC) from 0 to 180 min, and the eGI value was calculated according to the following formula:

$$\mathrm{eGI} = 8.198 + 0.862\mathrm{HI}$$

3

2.7 Statistical analysis

Through SPSS 27.0 statistical software, one-way analysis of variance was used to test the significance of differences. Meanwhile, Duncan was applied to conduct multiple comparisons of the data. The results were expressed as mean ± standard deviation (SD). When $p < 0.05$, the difference was considered significant. Plot based on data using Origin 2018 software; The crystallinity was analyzed by MDI Jade 6 software.

3 Results and discussion

3.1 Physical properties of RS_3

3.1.1 RS content

The physical properties of RS_3 are presented in Table 1. As a specialized high-amylose cultivar, Youtang rice inherently contains a substantial amount of RS_2 (Yang et al., 2023). Consequently, the initial RS content of rice starch reached 11.63%. Although RS_2 readily degrades under the high temperatures required for RS_3 preparation due to its poor thermal stability, the high amylose content facilitates RS_3 formation during the subsequent retrogradation and recrystallization process (Q. Liu et al., 2025; Magallanes-Cruz et al., 2020). The treatment with α-amylase and pullulanase markedly elevated the RS yield. Following the sequential gelatinization - enzymolysis - retrogradation process, the RS contents of RS_3 derived from all staple food sources were significantly higher than those of their native counterparts. Among the tested sources, maize RS_3 exhibited the highest RS content, reaching 35.28%.

The content of amylose is usually positively correlated with the RS content in the prepared RS_3 (Margareta Leeman et al., 2006). During retrogradation, a higher amylose content favors the formation of double-helical structures, thereby enhancing recrystallization efficiency. The main chains of amylopectin consist of glucose units linked by α-1,4-glycosidic bonds, with branches connected via α-1,6 glycosidic bonds, forming a dendritic structure (Tian & Sun, 2020). As previously mentioned, pullulanase specifically hydrolyzes the α-1,6 linkages at the branching points of starch, effectively removing side chains and increasing the proportion of amylose. Meanwhile, α-amylase randomly cleaves α-1,4 glycosidic bonds along starch chains. Zhang et al. further reported that α-amylase preferentially hydrolyzes the internal regions of the starch backbone (B. Zhang et al., 2013).

Table 1
Physical properties of RS_3

Samples	RS Content (%)	Crystallization Type	Crystallinity (%)	Swelling power (g/g)	Solubility (%)
Wheat Starch	1.27 ± 0.01^{f}	A	20.15	14.96 ± 0.23^{a}	19.65 ± 0.41^{d}
Rice Starch	11.63 ± 0.70^{d}	A + B	37.24	11.48 ± 0.06^{b}	9.64 ± 0.38^{f}
Maize Starch	5.37 ± 0.01^{e}	A	23.76	12.94 ± 0.42^{c}	11.84 ± 0.52^{e}
Wheat RS_3	22.43 ± 0.77^{c}	B + V	43.31	6.90 ± 0.16^{d}	31.65 ± 0.21^{c}
Rice RS_3	30.27 ± 0.72^{b}	B + V	40.26	6.02 ± 0.19^{e}	35.69 ± 0.43^{b}
Maize RS_3	35.28 ± 0.28^{a}	B + V	46.13	5.81 ± 0.21^{e}	37.90 ± 0.34^{a}

3.1.2 Swelling power and solubility

The water absorption capacity of starch is primarily reflected by its swelling power (Zhuang et al., 2024). When starch is heated above its gelatinization temperature, water molecules form hydrogen bonds with the hydroxyl groups along the starch chains, inducing granule swelling. When starch is heated above its gelatinization temperature, water molecules form hydrogen bonds with the hydroxyl groups along the starch chains, inducing granule swelling (Jan et al., 2016). As shown in Table 1, following the gelatinization - enzymolysis - retrogradation treatment, the swelling power of RS_3 samples derived from various staple grains was significantly reduced and negatively correlated with RS content, with maize RS_3 exhibiting the lowest value (5.81 g/g). Enzymatic debranching substantially increases the

proportion of amylose, which has been reported to inhibit granule swelling and restrict the disruption of the double-helical structure of amylopectin (Jayakody & Hoover, 2008). This phenomenon aligns with the swelling behavior observed in native starches, where native rice starch exhibited the lowest swelling power (11.94 g/g) owing to its naturally higher amylose content.

The solubility of RS_3 samples was significantly increased, indicating extensive degradation of native starch structures. Indeed, the degree of solubility directly reflects the extent of starch component breakdown (X. Wang et al., 2018). As presented in Table 1, native starches exhibited much lower solubility, which is consistent with the findings of Obadi et al., who reported that higher amylose content in native starch naturally restricts its solubility (Obadi et al., 2023). During RS_3 preparation, enzymatic hydrolysis selectively disrupted the amorphous regions of starch, thereby markedly enhancing the solubility of the resulting RS_3 samples.

3.2 Structural properties of RS_3

3.2.1 FTIR

Figure 1a displays the FT-IR spectra of native starches from various staple grains alongside their corresponding RS_3 samples. The broad absorption band at 3400 cm^{-1} usually represents -OH stretching and hydrogen bond vibrations (Lian et al., 2014). Compared with native starches, the RS_3 samples exhibited broader and smoother peaks, with maize RS_3 showing the most pronounced attenuation. The peak at 2930 cm^{-1}, corresponding to asymmetric C-H stretching vibrations, weakened to varying degrees in RS_3. This indicates partial cleavage of C-H bonds following the gelatinization-enzymolysis-retrogradation process (Zou et al., 2020). The absorption peak around 1645 cm^{-1} corresponds to the bending vibrations of bound water within the starch matrix; its attenuation in RS_3 suggests a rearrangement of structural water and tight molecular packing during retrogradation (M. Wang et al., 2023). Additionally, the band at 1080 cm^{-1}, associated with C-O and C-H vibrations, exhibited significantly higher intensity in RS_3 than in native starches (M. Wang et al., 2023). Notably, no new absorption peaks emerged in RS_3 derived from different staple food sources, indicating that the enzymatic and physical modifications did not introduce new functional groups or chemical bonds, but rather altered the physical spatial arrangement of the molecules. During retrogradation, enhanced intermolecular hydrogen bonding contributed to a more ordered crystalline structure, as hydrogen bonding strength directly reflects short-range molecular order (Lu et al., 2023). Among all samples, maize RS_3 exhibited the highest degree of structural order and interchain binding ability. This heightened order is likely attributed to the enriched proportion of short-chain amylose produced during enzymatic debranching, which actively promotes recrystallization (Zou et al., 2020).

3.2.2 XRD

The XRD patterns of native starches from various staple grains and their corresponding RS_3 samples are shown in Fig. 1b. Native wheat and maize starches exhibited typical A-type crystalline structures, characterized by prominent diffraction peaks at 2θ = 15.0°, 17.0°, 18.0° and 23.0°. In contrast, native rice starch displayed distinct peaks near 2θ = 15.0°, 18.0°, 23.0°, and 24.0°, reflecting a mixed A- and B-type polymorph. Following processing, the RS_3 samples exhibited a mixed B + V-type crystalline structure, with major diffraction peaks at 2θ = 15.0°, 17.0°, 20.0° and 24.0°. Enzymatic treatment markedly altered the crystallization behavior of starch, primarily driven by modifications in its underlying molecular structure. Enzymatic debranching cleaved long starch chains, thereby increasing the proportion of short linear amylose chains and elevating the relative amylose content. These structural modifications facilitated the formation of a dense crystalline matrix with enhanced enzymatic resistance during the retrogradation process. As

summarized in Table 1, the relative crystallinity of all RS_3 samples increased significantly following the gelatinization - enzymolysis - retrogradation process. Maize RS_3 exhibited the highest crystallinity (46.13%), followed by wheat RS_3 (43.31%) and rice RS_3 (40.26%). This indicates that maize starch possesses the highest recrystallization efficiency under identical preparation conditions. The overall increase in crystallinity is primarily driven by molecular reorganization during retrogradation, which leads to a thorough restructuring of crystalline and amorphous regions into a thermodynamically stable configuration (M. Wang et al., 2023). The elevated crystallinity directly enhances the resistance of starch granules to digestive enzymes, showing a positive correlation. This observation is mutually supported by the FTIR spectroscopic analysis.

3.3 SEM

The SEM micrographs in Fig. 2 illustrate the surface morphology of native starches from the three staple grains and their corresponding RS_3 samples. Native starch morphology varied considerably depending on the botanical source. Native wheat starch exhibited bimodal granule size distribution, where large granules presented smooth, disk-like or lenticular shapes, while small granules displayed irregular or spherical geometries. Rice starch granules were smaller than those of wheat and maize, appearing irregular or polyhedral with sharp edges and smooth surfaces lacking visible pores. Maize starch granules exhibited a morphology similar to that of rice starch, predominantly featuring polyhedral shapes with sharp, defined edges. After the gelatinization–enzymolysis–retrogradation process, the morphology of RS_3 samples underwent substantial changes. The native granular architecture was completely destroyed, liberating linear amylose chains. During retrogradation, these chains recrystallized into a novel hierarchical network characterized by rough, porous, and folded surface structures, with adjacent particles agglomerating into large, fragmented aggregates. Following gelatinization, enzymatic treatment with α-amylase and debranching by pullulanase significantly increased the proportion of short-chain amylose, which has a high propensity for crystallization. This promoted the formation of more compact and ordered crystalline structures during retrogradation, thereby enhancing the resistance of RS_3 to enzymatic hydrolysis (H. Zhang et al., 2013).

The images of the control and three RS_3-supplemented groups are also presented in Fig. 2. Evidently, the control sample made from regular rice flour exhibited a rough, irregular surface with numerous dispersed fine fragments. In contrast, the extruded rice samples fortified with RS_3 from different staple grains displayed noticeably smoother and more continuous surface architectures. Among them, ER-4, which contains the highest level of RS, showed the finest and most delicate surface morphology. The thermal and mechanical shear forces during extrusion optimized the melt rheology of the flour matrix, thereby facilitating a more homogeneous fusion among the structural components. Similarly, previous research demonstrated that incorporating RS_3 into noodle matrices significantly enhanced their cross-sectional compactness (Si et al., 2024). Likewise, the addition of RS_3 in this study fortified the structural integrity of the extruded rice, yielding a denser and more uniform internal texture.

3.4 Pasting properties

As presented in Table 2, the peak viscosity of extruded rice formulated with RS_3 from different staple grains was significantly lower than that of the control. This decrease is primarily attributed to the presence of RS_3, which restricted starch granule swelling and gelatinization during heating. Among all formulations, sample ER-4 exhibited the lowest peak viscosity. Furthermore, the uniform distribution of RS_3 with rice starch granules may contribute to the formation of a more compact structure, which significantly reduced the breakdown values of the RS_3-supplemented extruded rice. However, no significant differences in breakdown values were observed among the three experimental groups. Breakdown values generally reflect the the thermal stability of starch under heating and shear, and the data showed in Table 2 indicated that the thermal stability of extruded rice has significantly improved by the addition of

RS_3. Setback values generally reflect the short-term retrogradation tendency of starch. Previous studies have shown that when the setback value is positive and increased, the texture of rice tended to become harder and coarser. In contrast, a negative setback value is usually associated with an overly sticky texture (Limpisut & Jindal, 2002). In this study, the addition of RS_3 significantly increased the setback values of the extruded rice. Among all formulations, the setback value of ER-4, which had the highest content of RS_3, was significantly higher than that of the other three groups. A moderate increase in setback value promotes the formation of a cohesive surface layer during cooking, thereby enhancing grain structural integrity and visual clarity in cooked rice.

Table 2
Pasting properties of extruded rice

Sample	Peak viscosity(cP)	Trough viscosity(cP)	Breakdown(cP)	Final viscosity(cP)	Setback(cP)
ER-1	86.50 ± 0.65^{a}	30.32 ± 1.28^{a}	56.30 ± 1.71^{a}	56.32 ± 0.84^{a}	-30.06 ± 0.75^{c}
ER-2	15.52 ± 1.05^{b}	11.32 ± 0.75^{c}	2.45 ± 0.63^{b}	35.71 ± 0.86^{b}	16.74 ± 0.26^{b}
ER-3	14.02 ± 0.34^{b}	14.00 ± 0.26^{b}	2.98 ± 0.76^{b}	33.00 ± 0.95^{b}	17.50 ± 0.31^{b}
ER-4	10.41 ± 0.51^{c}	9.50 ± 0.81^{d}	2.57 ± 0.84^{b}	26.06 ± 1.41^{c}	19.29 ± 0.95^{a}

3.5 Cooking quality

The cooking quality of rice is primarily evaluated by two key metrics: water absorption and cooking loss. Water absorption reflects the hydration capacity of rice during cooking, expressed as the percentage mass increase. Meanwhile, the cooking loss rate measures the leaching of soluble nutrients, such as amylose and soluble proteins, reflecting the degree of structural integrity and nutrient retention within the starch matrix (Hu et al., 2023; Tang et al., 2013). As presented in Table 3, the addition of RS_3 significantly decreased the water absorption of extruded rice compared to the control, accompanied by a slight reduction in the cooking loss rate. The reduction in cooking loss rate is generally believed to be related to the increase in amylose content. A elevated amylose content fosters a denser molecular matrix within the rice grains, which curtails water penetration and granule swelling, thereby restricting the leaching of soluble solids and reducing total cooking loss (Ngo et al., 2023). The RS_3 also has the same property, which can reduce water absorption and the swelling of starch particles. Therefore, in all the treatments, the sample ER-4, which had the highest RS_3 content, showed the lowest water absorption rate and cooking loss.

Table 3
Cooking quality and textural propertiesof extruded rice

Sample	Water absorption rate (%)	Hardness (g)	Adhesiveness (g·sec)	Springiness	Cohesiveness	Chewiness	Cooking loss rate (%)
ER-1	205.13 ± 5.09^{a}	122.35 ± 15.86^{a}	-17.69 ± 5.87^{c}	0.95 ± 0.03^{a}	0.74 ± 0.03^{a}	107.18 ± 6.33^{b}	6.65 ± 1.46^{a}
ER-2	193.52 ± 2.65^{b}	133.00 ± 10.22^{a}	-28.28 ± 2.72^{b}	0.96 ± 0.0^{a}	0.72 ± 0.02^{a}	116.53 ± 19.72^{b}	5.72 ± 1.26^{a}
ER-3	169.16 ± 1.79^{c}	143.68 ± 32.56^{a}	-30.37 ± 3.26^{b}	0.96 ± 0.01^{a}	0.72 ± 0.01^{a}	123.81 ± 23.94^{b}	4.90 ± 2.18^{a}
ER-4	164.01 ± 2.58^{d}	148.72 ± 31.80^{a}	-41.09 ± 3.05^{a}	0.96 ± 0.01^{a}	0.73 ± 0.02^{a}	154.65 ± 28.77^{a}	4.67 ± 0.78^{a}

3.6 Texture properties

Textural properties are critical indicators for evaluating food quality and consumer acceptability. Key parameters such as hardness, springiness, adhesiveness, cohesiveness, and chewiness not only reflect the physical characteristics of food but are also closely related to sensory perception during consumption (H. Li & Gilbert, 2018). As presented in Table 3, although no statistically significant differences in hardness were observed among the extruded rice formulations, RS_3-supplemented samples consistently exhibited higher hardness values. Moreover, hardness positively correlated with the RS content derived from the different staple grains. Among them, the maize RS_3 incorporated into sample ER-4 possessed the highest RS content, resulting in the maximum hardness value for ER-4 (148.72 g). Additionally, RS_3 supplementation significantly improved the chewiness of extruded rice, with ER-4 again demonstrating the highest value (154.65 g). However, excessive RS_3 incorporation may induce undesirable hardness and compromise chewiness, ultimately impairing overall palatability (Aravind et al., 2013). Conversely, RS_3 addition significantly reduced the adhesiveness of the extruded rice, a parameter closely tied to structural integrity and surface stickiness. This reduction occurs because RS_3 possesses high thermal stability, which limits starch gelatinization during extrusion; furthermore, dietary fiber within the raw materials may complex with proteins, thereby reducing melt viscosity (Beck et al., 2018). According to Wee et al., springiness increases with protein content (Wee et al., 2018). As the protein contents of the four extruded rice groups were similar, no significant differences in springiness were observed.

3.7 Sensory evaluation

Table 4 presents the sensory evaluation results for the four groups of extruded rice, which were comprehensively assessed across five attributes: odor, appearance and structure, palatability, taste, and cold rice texture. As indicated in Table 3, all extruded rice samples received relatively low odor scores. This can likely be attributed to the thermal degradation and volatilization of volatile flavor compounds during high-temperature and high-pressure extrusion (Y. Liu et al., 2024). Compared to the control, the luster scores of the extruded rice with the addition of RS_3 were lower, with the lowest score for ER-2. It was evident that with the addition of RS_3, the integrity, stickiness and hardness of the rice kernels of ER-2, ER-3 and ER-4 were improved. Notably, sample ER-4, which contained maize RS_3 with the highest resistant starch content, achieved the highest overall sensory score (81).

Table 4
The sensory results of extruded rice

Sample	Odor	Appearance structure			Palatability			Taste	Cold rice texture	Total score
		Color	Luster	Integrity of rice grains	Stickiness	Elasticity	Hardness			
ER-1	15.3	5.2	5.8	4.1	6.9	6.4	7.4	23.8	3.2	78.1
ER-2	15.4	4.0	5.2	4.5	7.8	6.5	8.6	23.4	3.5	78.9
ER-3	15.6	4.2	5.6	4.6	8.1	6.7	8.8	23.6	3.7	80.8
ER-4	15.5	4.5	5.4	4.6	8.3	6.7	9.1	23.2	3.7	81

3.8 eGI

As shown in Fig. 3a, the in vitro digestibility of all four groups of extruded rice ER-1 (55.96%), ER-2 (37.50%), ER-3 (35.16%) and ER-4 (34.32%) were significantly lower than that of white bread (73.62%). The digestion kinetics followed

a similar pattern across all samples, characterized by a rapid phase during the first hour, followed by a slower increase until reaching a plateau. The calculated eGI values are summarized in Fig. 3b. The eGI values of ER-1 (74.36), ER-2 (50.22), ER-3 (47.46), and ER-4 (45.88) were significantly lower than that of the white bread (100). Crucially, the eGI values of ER-2, ER-3, and ER-4 were all less than 55, classifying them as low-GI foods with strong digestion resistance and potential hypoglycemic benefits, with maize RS_3-fortified ER-4 achieving the lowest value. Conversely, ER-1 was classified as a high-GI food. This high value likely stems from the intensive thermal and mechanical forces during milling and extrusion, which rendered starch molecules more susceptible to gelatinization and fully uncoiled molecular chains, thereby exposing more catalytic sites to digestive enzymes (Y. Liu et al., 2024). In contrast, ER-2, ER-3, and ER-4 resisted enzymatic breakdown due to their elevated RS_3 content, which enhanced resistance to hydrolysis and suppressed the rate of starch degradation, ultimately yielding significantly lower eGI values (Brighenti et al., 2006).

4 Conclusion

This study investigated the preparation and physicochemical properties of RS_3 derived from three staple grains (wheat, rice, and maize). The resulting RS_3 samples exhibited marked variations in RS content, crystallinity, swelling power, and solubility. Enzymatically prepared RS_3 showed substantially higher RS content than native starch, with maize RS_3 achieving the highest value (35.28%), indicating a superior recrystallization efficiency of maize starch during retrogradation. FTIR spectra revealed no shift in chemical functional groups, whereas XRD analysis confirmed a structural transition toward denser B- and V-type crystalline polymorphs. Furthermore, RS_3 formation significantly decreased swelling power but increased solubility. The increased proportion of short amylose chains restricted the hydration and expansion of starch granules.

The results of pasting properties and textural properties show that incorporating RS_3 markedly enhanced the texture of the extruded rice while reducing water absorption and cooking loss. Compared with the control, RS_3-fortified extruded rice received higher overall acceptability, with the maize RS_3 formulation (ER-4) achieving the highest sensory score (81). Additionally, RS_3 fortification substantially decreased the eGI of extruded rice. The eGI values for all RS_s-added samples were less than 55, with the ER-4 exhibiting the lowest eGI (45.88) and superior resistance to enzymatic digestion. These results can provide a reference for the development of low-GI foods using the RS_3 derived from staple grains.

Abbreviations

Glycemic Index
GI
Resistant Starch
RS
Estimated Glycemic Index
eGI
Fourier Transform Infrared
FTIR
X-ray Diffraction
XRD
Scanning Electron Microscopy
SEM
Rapid Visco Analyzer

RVA
Hydrolysis Index
HI
Area Under the Curve
AUC

Declarations

Declaration of Competing Interest

The authors declare no competing financial interests.

Funding

This research was funded by the Shanghai Agricultural Science and Technology Innovation Project, grant number V2025004; the Shanghai Agriculture Applied Technology Development Program, grant number I2023007; the Shanghai agricultural products preservation and processing professional technical service platform, grant number 21 DZ2292200; the Shanghai agricultural products preservation and processing engineering technology research center, grant number 19 DZ2251600; and the Natural Science Foundation of China, great number 32201978.

CRediT authorship contribution statement

Songheng Wu: Writing - review & editing, Methodology, Conceptualization; **Haoyu Si**: Writing - original draft, Investigation, Data Curation; **Kai Zhu:** Software, Validation; **Xing Jia:** Methodology, Visualization; **Qi Zheng:** Validation, Visualization; **Wenhui Tian:** Methodology, Formal analysis; **Yuemei Zhang:** Validation; **Hongzhu Chen:** Methodology, Resources; **Ruihan Lin:** Methodology; **Yongjin Qiao**: Resources, Funding acquisition; **Yi Zhang**: Methodology, Funding acquisition, Project administration.

Declaration of Competing Interest

The authors declare no competing financial interests.

Data availability

The data presented in this study are available on request from the corresponding author. The data are not publicly available due to privacy.

Human Ethics and Consent to Participate declarations

Not applicable.

References

1. Aravind, N., Sissons, M., Fellows, C. M., Blazek, J., & Gilbert, E. P. (2013). Optimisation of resistant starch II and III levels in durum wheat pasta to reduce in vitro digestibility while maintaining processing and sensory characteristics. *Food Chemistry*, *136*(2), 1100–1109. https://doi.org/10.1016/j.foodchem.2012.08.035
2. Arp, C. G., Correa, M. J., & Ferrero, C. (2020). Production and Characterization of Type III Resistant Starch from Native Wheat Starch Using Thermal and Enzymatic Modifications. *Food and Bioprocess Technology*, *13*(7), 1181–1192. https://doi.org/10.1007/s11947-020-02470-5

3. Beck, S. M., Knoerzer, K., Foerster, M., Mayo, S., Philipp, C., & Arcot, J. (2018). Low moisture extrusion of pea protein and pea fibre fortified rice starch blends. *Journal of Food Engineering*, *231*, 61–71. https://doi.org/10.1016/j.jfoodeng.2018.03.004
4. Brighenti, F., Benini, L., Del Rio, D., Casiraghi, C., Pellegrini, N., Scazzina, F., Jenkins, D. J., & Vantini, I. (2006). Colonic fermentation of indigestible carbohydrates contributes to the second-meal effect. *The American Journal of Clinical Nutrition*, *83*(4), 817–822. https://doi.org/10.1093/ajcn/83.4.817
5. Deng, W., Zhao, L., Chen, C., Ren, Z., Jing, Y., Qiu, J., & Liu, D. (2024). National burden and risk factors of diabetes mellitus in China from 1990 to 2021: Results from the Global Burden of Disease study 2021. *Journal of Diabetes*, *16*(10), e70012. https://doi.org/10.1111/1753-0407.70012
6. Gong, X., Qiu, Q., Zong, M., Zhong, Y., Sun, D., Yi, J., & Wang, T. (2026). Tricholoma matsutake root by-product improves flavor and functionality of extruded reconstructed rice. *Journal of Cereal Science*, *130*, 104484. https://doi.org/10.1016/j.jcs.2026.104484
7. Hu, F., Li, J.-Y., Zou, P.-R., Thakur, K., Zhang, J.-G., Khan, M. R., & Wei, Z.-J. (2023). Effects of Lycium barbarum on gluten structure, in vitro starch digestibility, and compound noodle quality. *Food Bioscience*, *54*, 102915. https://doi.org/10.1016/j.fbio.2023.102915
8. Jan, R., Saxena, D. C., & Singh, S. (2016). Pasting, thermal, morphological, rheological and structural characteristics of Chenopodium (Chenopodium album) starch. *LWT - Food Science and Technology*, *66*, 267–274. https://doi.org/10.1016/j.lwt.2015.10.040
9. Jayakody, L., & Hoover, R. (2008). Effect of annealing on the molecular structure and physicochemical properties of starches from different botanical origins – A review. *Carbohydrate Polymers*, *74*(3), 691–703. https://doi.org/10.1016/j.carbpol.2008.04.032
10. Li, H., & Gilbert, R. G. (2018). Starch molecular structure: The basis for an improved understanding of cooked rice texture. *Carbohydrate Polymers*, *195*, 9–17. https://doi.org/10.1016/j.carbpol.2018.04.065
11. Li, M., Li, H., Dai, L., Zhou, L., McClements, D. J., Sun, Q., & Xiong, L. (2026). Synergistic construction of heat-stable resistant starch by confined Retrogradation of short-chain amylose within calcium alginate beads. *Food Chemistry*, *520*, 149803. https://doi.org/10.1016/j.foodchem.2026.149803
12. Lian, X., Wang, C., Zhang, K., & Li, L. (2014). The retrogradation properties of glutinous rice and buckwheat starches as observed with FT-IR, 13C NMR and DSC. *International Journal of Biological Macromolecules*, *64*, 288–293. https://doi.org/10.1016/j.ijbiomac.2013.12.014
13. Liao, H.-J., Lai, P.-Y., Koh, Y.-C., & Hung, C.-C. (2016). Physicochemical characteristics and in vitro digestibility of *indica*, *japonica*, and waxy type rice flours and their derived resistant starch type III products: Physicochemical and characteristics and in vitro digestibility of rice flours. *Starch - Stärke*, *68*(5–6), 462–468. https://doi.org/10.1002/star.201500319
14. Limpisut, P., & Jindal, V. K. (2002). Comparison of Rice Flour Pasting Properties using Brabender Viscoamylograph and Rapid Visco Analyser for Evaluating Cooked Rice Texture. *Starch - Stärke*, *54*(8), 350–357. https://doi.org/10.1002/1521-379X(200208)54:8%3C350::AID-STAR350%3E3.0.CO;2-R
15. Liu, Q., Xia, Z., Guan, H., Jiao, A., Ge, S., Wang, D., Yu, Y., & Jin, Z. (2025). A review on the comparison of preparation, structure and properties of two types of resistant starch type III formed from long and short-chain amylose. *Trends in Food Science & Technology*, *166*, 105388. https://doi.org/10.1016/j.tifs.2025.105388
16. Liu, Y., Ma, Q., Yan, J., Luo, Z., Zhang, Y., & Wang, J. (2024). Preparation and characterization of extruded rice with a low glycemic index (in Chinese). *Modern Food Science and Technology*, *40*(10), 40–49.
17. Lu, H., Tian, Y., & Ma, R. (2023). Assessment of order of helical structures of retrograded starch by Raman spectroscopy. *Food Hydrocolloids*, *134*, 108064. https://doi.org/10.1016/j.foodhyd.2022.108064

18. Luo, S., Zhou, B., Cheng, L., Huang, J., Zou, P., Zeng, Y., Huang, S., Chen, T., Liu, C., & Wu, J. (2022). Pre-fermentation of rice flour for improving the cooking quality of extruded instant rice. *Food Chemistry*, *386*, 132757. https://doi.org/10.1016/j.foodchem.2022.132757
19. Magallanes-Cruz, P. A., Bello-Pérez, L. A., Agama-Acevedo, E., Tovar, J., & Carmona-Garcia, R. (2020). Effect of the addition of thermostable and non-thermostable type 2 resistant starch (RS2) in cake batters. *LWT*, *118*, 108834. https://doi.org/10.1016/j.lwt.2019.108834
20. Margareta Leeman, A., Karlsson, M. E., Eliasson, A.-C., & Björck, I. M. E. (2006). Resistant starch formation in temperature treated potato starches varying in amylose/amylopectin ratio. *Carbohydrate Polymers*, *65*(3), 306–313. https://doi.org/10.1016/j.carbpol.2006.01.019
21. Ngo, T. V., Kunyanee, K., & Luangsakul, N. (2023). Insights into Recent Updates on Factors and Technologies That Modulate the Glycemic Index of Rice and Its Products. *Foods*, *12*(19), 3659. https://doi.org/10.3390/foods12193659
22. Noori, T., Sureda, A., & Shirooie, S. (2023). Role of natural mTOR inhibitors in treatment of diabetes mellitus. *Fundamental & Clinical Pharmacology*, *37*(3), 461–479. https://doi.org/10.1111/fcp.12851
23. Obadi, M., Qi, Y., & Xu, B. (2023). High-amylose maize starch: Structure, properties, modifications and industrial applications. *Carbohydrate Polymers*, *299*, 120185. https://doi.org/10.1016/j.carbpol.2022.120185
24. Pang, J., Zhang, Y., Song, X., Tong, X., Wu, S., Hu, Y., Zhong, Y., & Qiao, Y. (2024). Molecular characterization, rheological properties, and prebiotic properties of arabinoxylans from waxy and sweet corn cobs. *Cereal Chemistry*, *101*(3), 493–507. https://doi.org/10.1002/cche.10747
25. Ratnaningsih, N., Suparmo, Harmayani, E., & Marsono, Y. (2020). Physicochemical properties, in vitro starch digestibility, and estimated glycemic index of resistant starch from cowpea (Vigna unguiculata) starch by autoclaving-cooling cycles. *International Journal of Biological Macromolecules*, *142*, 191–200. https://doi.org/10.1016/j.ijbiomac.2019.09.092
26. Romero-Bastida, C. A., Bello-Pérez, L. A., García, M. A., Martino, M. N., Solorza-Feria, J., & Zaritzky, N. E. (2005). Physicochemical and microstructural characterization of films prepared by thermal and cold gelatinization from non-conventional sources of starches. *Carbohydrate Polymers*, *60*(2), 235–244. https://doi.org/10.1016/j.carbpol.2005.01.004
27. Schmidt, M., Begemann, J., Weber, L., Gattner, C., & Smit, I. (2023). Genotype specific starch characteristics in relation to resistant starch formation in table potatoes. *Food & Function*, *14*(15), 7096–7108. https://doi.org/10.1039/D3FO01626A
28. Si, H., Xie, F., Yang, R., Gu, W., Wu, S., Zhang, J., Zhang, Y., & Qiao, Y. (2024). Recent developments in enzymatic preparation, physicochemical properties, bioactivity, and application of resistant starch type III from staple food grains. *International Journal of Biological Macromolecules*, *279*, 135521. https://doi.org/10.1016/j.ijbiomac.2024.135521
29. Simsek, S., & El, S. N. (2012). Production of resistant starch from taro (Colocasia esculenta L. Schott) corm and determination of its effects on health by in vitro methods. *Carbohydrate Polymers*, *90*(3), 1204–1209. https://doi.org/10.1016/j.carbpol.2012.06.039
30. Stewart, M., Wilcox, M., Bell, M., Buggia, M., & Maki, K. (2018). Type-4 Resistant Starch in Substitution for Available Carbohydrate Reduces Postprandial Glycemic Response and Hunger in Acute, Randomized, Double-Blind, Controlled Study. *Nutrients*, *10*(2), 129. https://doi.org/10.3390/nu10020129
31. Tang, M., Hong, Y., Gu, Z., Zhang, Y., & Cai, X. (2013). The effect of xanthan on short and long-term retrogradation of rice starch. *Starch - Stärke*, *65*(7–8), 702–708. https://doi.org/10.1002/star.201200170

32. Tian, S., & Sun, Y. (2020). Influencing factor of resistant starch formation and application in cereal products: A review. *International Journal of Biological Macromolecules*, *149*, 424–431. https://doi.org/10.1016/j.ijbiomac.2020.01.264
33. Walker, K. Z., O'Dea, K., Gomez, M., Girgis, S., & Colagiuri, R. (2010). Diet and exercise in the prevention of diabetes. *Journal of Human Nutrition and Dietetics*, *23*(4), 344–352. https://doi.org/10.1111/j.1365-277X.2010.01061.x
34. Wang, M., Liu, G., Li, J., Wang, W., Hu, A., & Zheng, J. (2023). Structural and physicochemical properties of resistant starch under combined treatments of ultrasound, microwave, and enzyme. *International Journal of Biological Macromolecules*, *232*, 123331. https://doi.org/10.1016/j.ijbiomac.2023.123331
35. Wang, X., Reddy, C. K., & Xu, B. (2018). A systematic comparative study on morphological, crystallinity, pasting, thermal and functional characteristics of starches resources utilized in China. *Food Chemistry*, *259*, 81–88. https://doi.org/10.1016/j.foodchem.2018.03.121
36. Wee, M. S. M., Goh, A. T., Stieger, M., & Forde, C. G. (2018). Correlation of instrumental texture properties from textural profile analysis (TPA) with eating behaviours and macronutrient composition for a wide range of solid foods. *Food & Function*, *9*(10), 5301–5312. https://doi.org/10.1039/C8FO00791H
37. Wu, J., Chen, J., Liu, W., Liu, C., Zhong, Y., Luo, D., Li, Z., & Guo, X. (2016). Effects of aleurone layer on rice cooking: A histological investigation. *Food Chemistry*, *191*, 28–35. https://doi.org/10.1016/j.foodchem.2014.11.058
38. Xing, J., Liu, Y., Li, D., Wang, L., & Adhikari, B. (2017). Heat-moisture treatment and acid hydrolysis of corn starch in different sequences. *LWT - Food Science and Technology*, *79*, 11–20. https://doi.org/10.1016/j.lwt.2016.12.055
39. Yang, R., Tang, J., Zhao, Q., Piao, Z., Lee, G., Wan, C., & Bai, J. (2023). Starch Properties of Roasting Rice from Naturally High-Resistant Starch Rice Varieties. *Molecules*, *28*(17), 6408. https://doi.org/10.3390/molecules28176408
40. Zhang, B., Dhital, S., & Gidley, M. J. (2013). Synergistic and Antagonistic Effects of α-Amylase and Amyloglucosidase on Starch Digestion. *Biomacromolecules*, *14*(6), 1945–1954. https://doi.org/10.1021/bm400332a
41. Zhang, H., Tian, Y., Bai, Y., Xu, X., & Jin, Z. (2013). Structure and properties of maize starch processed with a combination of α-amylase and pullulanase. *International Journal of Biological Macromolecules*, *52*, 38–44. https://doi.org/10.1016/j.ijbiomac.2012.09.030
42. Zhang, Y. (2022). Formula Optimization and Edible Quality Evaluation of Low GI Extruded Rice (in Chinese). *Journal of the Chinese Cereals and Oils Association*, *37*(03), 1. https://doi.org/10.3969/j.issn.1003-0174.2022.03.002
43. Zhuang, Y., Wang, Y., & Yang, H. (2024). Effects of cation valence on swelling power, solubility, pasting, gel strength characteristics of potato starch. *Food Chemistry*, *434*, 137510. https://doi.org/10.1016/j.foodchem.2023.137510
44. Zou, J., Xu, M., Wen, L., & Yang, B. (2020). Structure and physicochemical properties of native starch and resistant starch in Chinese yam (Dioscorea opposita Thunb.). *Carbohydrate Polymers*, *237*, 116188. https://doi.org/10.1016/j.carbpol.2020.116188

Figures

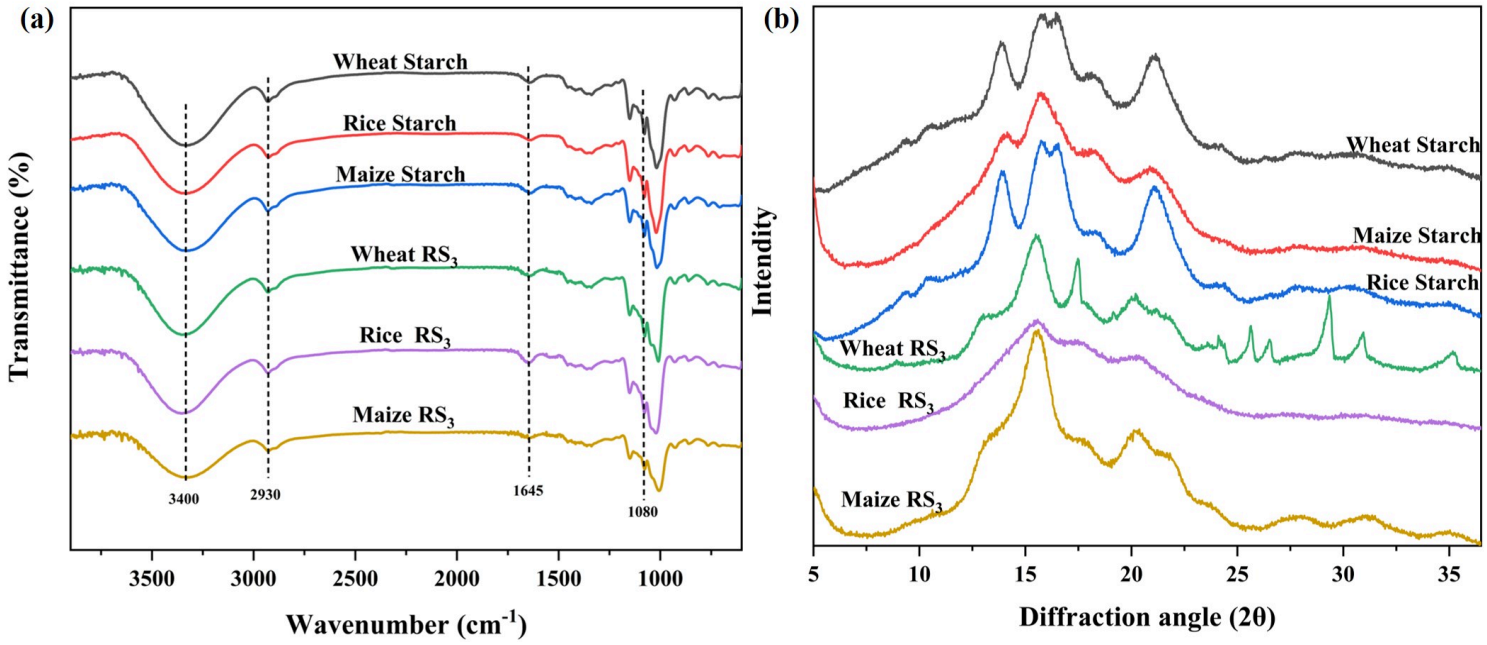


Figure 1

FTIR spectra and XRD patterns of starch and corresponding RS_3 from different source

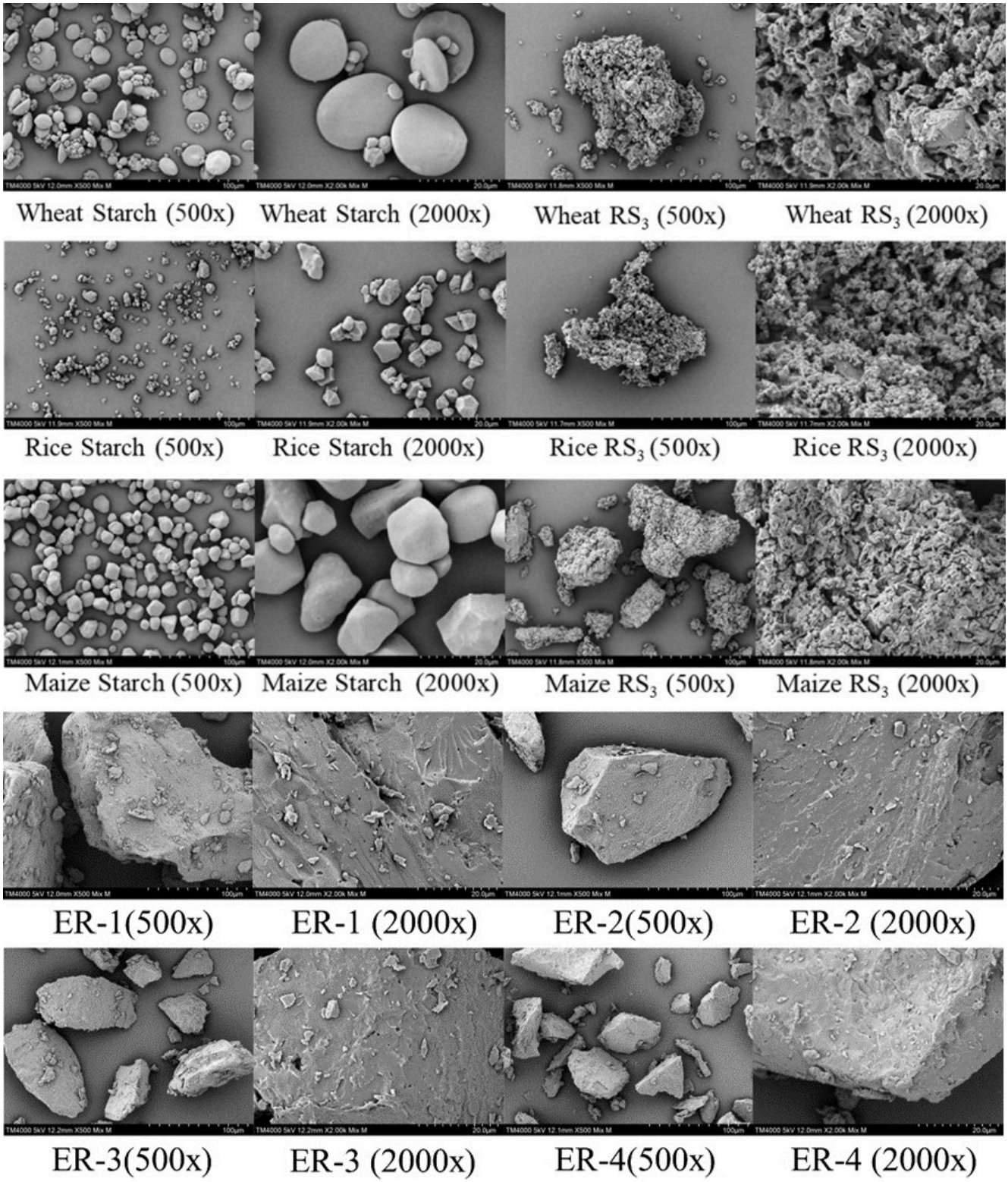


Figure 2

SEM images of RS_3 and extruded rice

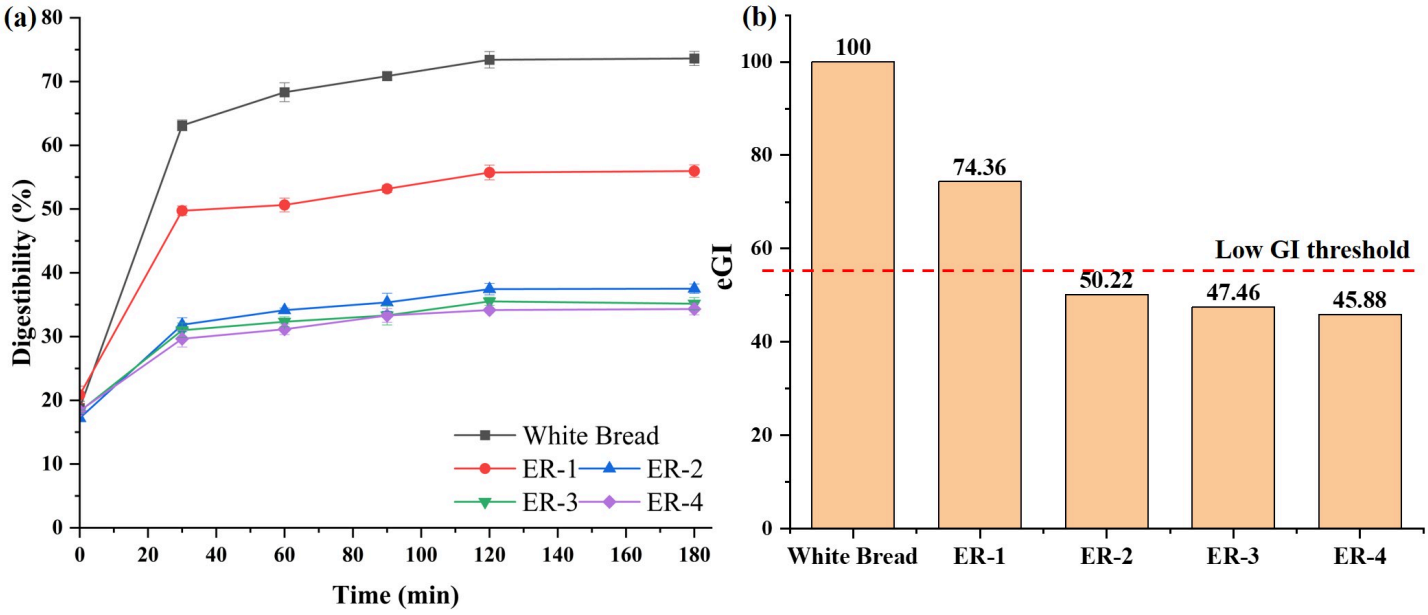


Figure 3

In vitro digestion curve and eGI values of extruded rice and white bread